Effects of thickness stretching in functionally graded plates and shells

Effects of thickness stretching in functionally graded plates and shells

E. Carrera *, S. Brischetto, M. Cinefra, M. Soave

Department of Aeronautics and Space Engineering, Politecnico di Torino, Italy

A B S T R A C T

The present work evaluates the effect of thickness stretching in plate/shell structures made by materials which are functionally graded (FGM) in the thickness directions. That is done by removing or retaining the transverse normal strain in the kinematics assumptions of various refined plate/shell theories. Variable plate/shell models are implemented according to Carrera's Unified Formulation. Plate/shell theories with constant transverse displacement are compared with the corresponding linear to fourth order of expansion in the thickness direction ones. Single-layered and multilayered FGM structures have been analyzed. A large numerical investigation, encompassing various plate/shell geometries as well as various grading rates for FGMs, has been conducted. It is mainly concluded that a refinements of classical theories that include additional in-plane variables could results meaningless unless transverse normal strain effects are taken into account.

1. Introduction

Functionally graded materials (FGMs) are multiphase composites with the volume fraction of phases varying through a direction. One advantage of FGMs compared to laminated composites is that the material properties continuously vary in the thickness direction, as opposed to being discontinuous across adjoining layers as they are in laminated composites. Such a peculiarities of FGM is in contrast with well know Kirchhoff–Love type plate/shell theories in which thickness stretching ϵ_{zz} is neglected and transverse displacement is considered independent by thickness coordinates. So called Koiter's Recommendation, see the discussion below, needs to be reconsidered. The numerical analysis of such a contrast is the topic of the present paper. However a general overview on FGM is for sake of completeness given along with the discussion plate/shell contribution which are relevant to this paper aims.

FGMs were first proposed in Japan, by materials scientists in the Sendai area, in 1984 [1], as thermal barrier materials. Since then, high-performance heat resistant barriers in FGMs have been developed. The FGM concept has also been considered to improve energy conversion efficiency. For other application fields, readers can refer to the excellent review by Koizumi [2].

Many topics are of interest for a better understanding of the use of FGMs: – improved production techniques; – extension of the applications to new fields; – introduction of effective micromechanical models; – development of accurate structural models: beam, plate and shell refined theories. The attention of the present paper is therefore focused on the latter aspect. An accurate kinematic description of FGM plates and shells, with variable properties in the thickness direction, appears to be a key point for the analysis of their mechanical response. Many papers on FGM modeling have recently appeared. An interesting review paper has been provided by Birman and Byrd [3].

A three-dimensional solution for FGM plates, subjected to a transverse mechanical load, has been proposed by Kashtalyan [4] and this solution has been extended to a sandwich panel with a functionally graded core by Kashtalyan and Menshykova [5]. Zenkour [6] accounted for the static response of a simply supported functionally graded rectangular plate subjected to a transversal mechanical load. A generalized shear deformation theory, which neglects the transversal normal strain, has been used. In [7], Batra and Jin considered FGM plates which are obtained by changing the fiber orientation along the thickness coordinate z. A free vibration problem has been investigated via the Finite Element (FE) method. A first order shear deformation theory has been applied and different boundary conditions have been investigated. Qian et al. [8] analyzed the static deformations and free and forced vibrations of a thick rectangular functionally graded elastic plate using a high-order shear and normal deformable plate theory and a meshless local Petrov–Galerkin method; the effective material moduli have been computed using the Mori–Tanaka homogenization technique [9]. Ramirez et al. [10] presented a static analysis of an anisotropic, elastic plate composed of functionally graded materials. The solution was obtained using a discrete layer theory in combination with the Ritz method. The FE solution has been compared with the exact solution by Pan [11] for

a functionally graded rectangular composite laminate under simply supported edge conditions; Pan's solution extends Pagano's 3D solution [12,13] to functionally graded materials. A three-dimensional exact solution has been presented for free and forced vibrations of simply supported FGM rectangular plates in [14]. Thick and thin plates have been analyzed for arbitrary variations of the material properties in the thickness direction. Exact natural frequencies, displacements and stresses are used to assess the accuracy of the Classical Lamination Theory (CLT), the first-order shear deformation theory (FSDT) and a third-order shear deformation theory. An analytical solution for thermo-mechanical deformations of a simply supported FGM plate subjected to time-dependent thermal loads at the top and/or bottom surfaces is illustrated in [15]. In [16], a third-order shear deformation theory has been applied to the static analysis of an FGM plate. The plate material is made of two isotropic constituents with their volume fractions varying only in the thickness direction. The aspect ratio effects of the plate and the volume fractions of the constituents on the centroidal deflection have been scrutinized. An elastic, rectangular and simply supported, functionally graded material plate of medium thickness subjected to a transverse loading has been investigated in [17]. Three evaluations have been considered in z for the FGM properties: the volume fraction can be defined by a power-law, sigmoid or exponential function. The model is based on CLT and Fourier series expansion. A closed form solution has been given in Part I, while a comparison between FE and analytical solutions has been given in Part II. The free vibration problem of FGM plates has been presented in the case of magneto–electro-elastic fields in [18]. Bayat et al. [19] analyzed functionally graded rotating disks with variable thickness: they presented an elastic solution, and the material properties and disk thickness profile are assumed as two power-law distributions. The effects of the material grading index and the geometry of the disk on the stresses and displacements have been investigated. Chiba [20] studied the stochastic heat conduction analysis of a functionally graded annular disk with spatially random heat transfer coefficients, where the mean and variance of the temperature are analytically obtained on the upper and lower surfaces. Recently, carbon nanotubes have been applied in ceramic FGMs [21]. Multiwalled carbon nanotubes are considered as unique agents to fabricate nanostructure-controlled functionally graded alumina ceramics, where the FGM concept offers the potential of successfully linking conventional ceramics to their nanocomposites which contain a high concentration of carbon nanotubes. Haddadpour et al. [22] made a supersonic flutter prediction of functionally graded cylindrical shells using the Love shell theory and von Karman–Donnell type non-linearity, coupled with a linearized first-order piston theory. They investigated the effects of internal pressure and temperature rise on the flutter boundaries of a simply supported FGM cylinder with different values of the power-law index. Na and Kim [23] have studied the optimization of volume fractions for functionally graded panels, considering stress and critical temperature and using an 18-node solid element.

An accurate kinematic description of the problem variables in the thickness direction appears to be a key point for the analysis of the mechanical behavior of FGM plates. Carrera's Unified Formulation (CUF), proposed in [24–26], has been extended to FGMs in [27–30]. The generalized expansion, upon which the CUF is based, relies on a set of functions herein indicated as thickness functions. In this manner, CUF reduces a three-dimensional problem to a bi-dimensional one. At the same time, the order of expansion along the thickness of the plate is taken as a free parameter of the problem and it can be changed in a 1–4 range. As a result, an exhaustive variable kinematic model is obtained. Refined displacement models (both layer wise and equivalent single layer descriptions) have been developed in [27] for FGM plate geometries. In [28] advanced mixed models have been extended to FGM plates by including transverse stresses as primary variables as the displacements. In [29] the models developed in [27,28] have been employed to analyze multilayered plates embedding FGM layers, in particular the effects of an FGM core have been investigated in classical sandwich structures. Finally, CUF (both refined and mixed models) has been extended to FGM shell geometries in [30]. In [27–30] refined and advanced models have been compared with available 3D solutions and with classical two-dimensional models (CLT and FSDT), but no comparisons with higher-order models discarding transverse normal strain have been performed.

The previous review shows that most FGM structures are analyzed by referring to three-dimensional solutions, or to classical and higher-order two-dimensional theories which neglect thickness stretching. In these latter theories, the transverse displacement is considered constant in the thickness direction, as in Kirchhoff–Love type thin plate/shell theories. This appears quite inappropriate since FGM structures are characterized by a strong variation of properties in the thickness direction. To further substantiate this fact, Koiter's recommendation [31] is here proposed:

> *a refinement of Love's first approximation theories is indeed meaningless, in general, unless the effects of transverse shear and normal stresses are taken into account at the same time.*

Such a recommendation, which was originally given for plates and shells made of traditional metallic isotropic materials, should play a more relevant role in the case of FGM structures which are graded in the transverse thickness direction.

No works are available that make the role played by the transverse normal strain 'thickness stretching' in FGM plates/shells evident. The present paper aims to fill this gap. To do this, the CUF, developed in previous papers, is applied to various plate/shell problems, and equivalent single layer (ESL) theories (linear up-to fourth order of expansion in the thickness directions z) are compared by including and discarding the transverse normal strain ϵ_{zz} effect, as was done in [32,33] for traditional layered structures.

The paper has been organized as follows: the geometry of the plates and shells is given in Section 2; Hooke's law for FGMs is discussed in Section 3; theories discarding and including thickness stretching are described in Section 4; the numerical discussion is given in Section 5 and the conclusions are summarized in Section 6. The whole numerical analysis has been conducted by using *MUL2* software which is available at the Aeronautics and Space Engineering Department of Politecnico di Torino.

2. Geometry

Plates and shells are bi-dimensional structures in which one dimension, the thickness, is negligible with respect to the other two in-plane dimensions. A shell geometry is shown in Fig. 1; Ω is the reference shell surface with the two in-plane orthogonal curvilinear coordinates α and β, z is the thickness coordinate. R_α, R_β are the curvature radii. By introducing a subscript k, the shell geometry related to a given k^{th} layer is considered.

The plate coincides with the flat shell case; the Cartesian coordinate system is employed in this case:

$$\alpha = x, \quad \beta = y, \quad z = z, \quad R_\alpha = R_\beta = \infty. \tag{1}$$

A plate geometry is shown in Fig. 2. In the case of shells, u_α, u_β and u_z are the displacement components in the α, β and z directions, respectively. For plates, the three displacement components in the x, y and z directions are u_x, u_y and u_z, respectively.

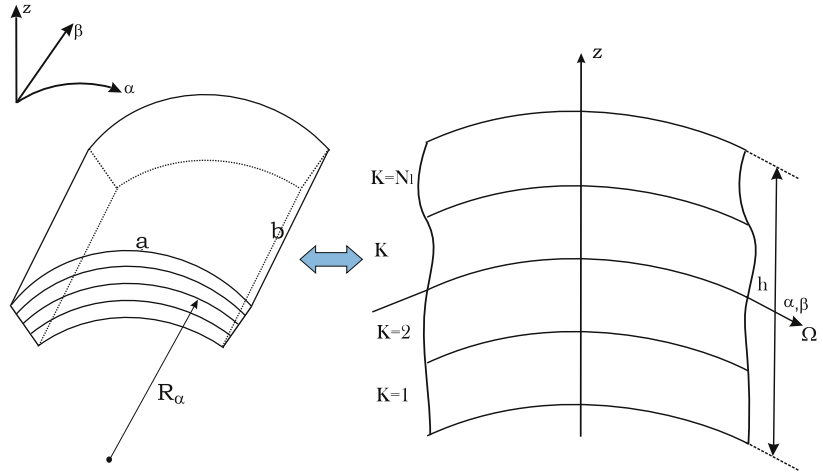

Fig. 1. Geometry and reference system for a multilayered shell.

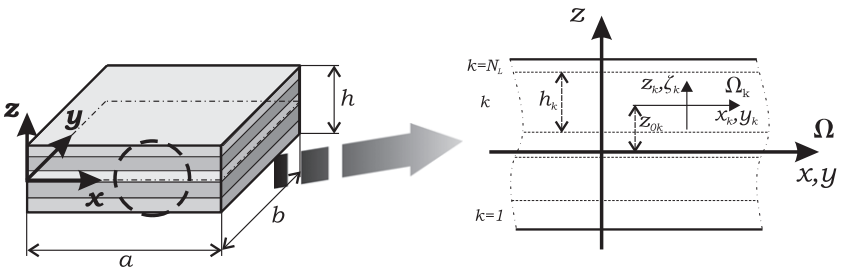

Fig. 2. Geometry and reference system for a multilayered plate.

3. Hooke's law for FGMs

Hooke's classical law for a layer k embedded in a multilayered structure is:

$$\boldsymbol{\sigma}_p^k = \mathbf{C}_{pp}^k \boldsymbol{\epsilon}_p^k + \mathbf{C}_{pn}^k \boldsymbol{\epsilon}_n^k, \tag{2}$$

$$\boldsymbol{\sigma}_n^k = \mathbf{C}_{np}^k \boldsymbol{\epsilon}_p^k + \mathbf{C}_{nn}^k \boldsymbol{\epsilon}_n^k, \tag{3}$$

where $\mathbf{C}_{pp}^k, \mathbf{C}_{pn}^k, \mathbf{C}_{np}^k, \mathbf{C}_{nn}^k$ are $[3 \times 3]$ sub-arrays containing the elastic coefficients for an orthotropic layer in the structure reference system [32–34]. The in-plane and out-plane stresses and strains, are $\boldsymbol{\sigma}_p^k = (\sigma_{\alpha\alpha}, \sigma_{\beta\beta}, \sigma_{\alpha\beta})^k, \boldsymbol{\sigma}_n^k = (\sigma_{\alpha z}, \sigma_{\beta z}, \sigma_{zz})^k$ and $\boldsymbol{\epsilon}_p^k = (\epsilon_{\alpha\alpha}, \epsilon_{\beta\beta}, \gamma_{\alpha\beta})^k$, $\boldsymbol{\epsilon}_n^k = (\gamma_{\alpha z}, \gamma_{\beta z}, \epsilon_{zz})^k$, respectively.

In the case of FGM layers, the coefficients in Eqs. (2) and (3) vary in the thickness direction z, according to a given law:

$$\mathbf{C}(z) = \mathbf{C}_0 * g(z), \tag{4}$$

where $\mathbf{C}_0$ is the reference stiffness matrix and $g(z)$ gives the variation along z. For convenience, the expansion in z is written as follows:

$$\mathbf{C}(z) = F_b(z)\mathbf{C}_b + F_t(z)\mathbf{C}_t + F_\gamma(z)\mathbf{C}_\gamma = F_r(z)\mathbf{C}_r \quad \text{with } r = 1, \ldots, 10, \tag{5}$$

where $\mathbf{C}_r$ are constant in z and the *thickness functions* F_r are a combination of Legendre polynomials [25,26]. F_b and F_t are the bottom and top values, respectively. F_γ are the higher-order terms. F_r coincide with those used in the Carrera's Unified Formulation for the Layer-Wise expansion cases [32–34].

4. Considered theories

Classical theories and higher-order theories including and discarding the transverse streching ϵ_{zz} are here presented for the most general case of shells including FGM layers. They simply degenerate into those for plates, as discussed in Section 2.

4.1. Theories discarding the transverse normal strain ϵ_{zz}

The thin plate/shell theory (or Classical Lamination Theory, CLT, for plates), based on assumptions made by Cauchy [35], Poisson [36] and Kirchhoff [37], discards transverse shear and through-the-thickness deformations. The displacement field related to this model is given in the form:

$$\begin{aligned} u_\alpha &= u_{0\alpha} - z\frac{\partial u_{0z}}{\partial \alpha}, \\ u_\beta &= u_{0\beta} - z\frac{\partial u_{0z}}{\partial \beta}, \\ u_z &= u_{0z}, \end{aligned} \tag{6}$$

where $u_{0\alpha}$, $u_{0\beta}$ and u_{0z} are the displacements of the mid-reference surface in the α, β and z directions, respectively, and $\frac{\partial}{\partial \alpha}$ and $\frac{\partial}{\partial \beta}$ are the partial derivatives with respect to the α and β directions, respectively. This displacement field states that the section remains plane and orthogonal to the shell reference surface Ω.

Transverse shear deformations are introduced according to the Reissner–Mindlin kinematic assumptions [38,39]:

$$\begin{aligned} u_\alpha &= u_{0\alpha} + z u_{1\alpha}, \\ u_\beta &= u_{0\beta} + z u_{1\beta}, \\ u_z &= u_{0z}. \end{aligned} \tag{7}$$

This theory is also called the first-order shear deformation theory, FSDT. Transverse shear stresses show an a priori constant piecewise distribution. $u_{1\alpha}$ and $u_{1\beta}$ are two additional degrees of freedom with respect to the model in Eq. (6). In both the CLT and FSDT cases, the Poisson locking phenomena is contrasted by means of the plane-stress conditions, as indicated in [40,41].

Higher-order theories (HOTs) which discard transverse normal strain, consider the same order of expansion in the thickness direction for the displacement components u_α and u_β:

$$\begin{aligned} u_\alpha &= u_{0\alpha} + zu_{1\alpha} + z^2u_{2\alpha} + \ldots + z^Nu_{N\alpha}, \\ u_\beta &= u_{0\beta} + zu_{1\beta} + z^2u_{2\beta} + \ldots + z^Nu_{N\beta}, \\ u_z &= u_{0z}, \end{aligned} \tag{8}$$

where N is the order of expansion, which is taken as a free parameter. In the numerical investigation, N is considered to be as low as 1 and as high as 4. HOTs are indicated with the acronyms $N = 1$ to $N = 4$, and it is specified that the transverse normal strain ϵ_{zz} is discarded. Poisson locking phenomena must be corrected as in the CLT and FSDT cases [40,41].

4.2. Theories including the transverse normal strain ϵ_{zz}

In HOTs which include transverse normal strains, the higher-order terms are introduced in the kinematic assumptions for the three displacement components. The third line of Eq. (8) is modified in order to consider the transverse normal strain:

$$u_z = u_{0z} + z^iu_{iz}, \quad \text{with } i = 1, \ldots, N. \tag{9}$$

In the considered implementation, the order of expansion N goes from 1 to 4, and the relative theories are indicated as $N = 1$ to $N = 4$.

5. Numerical results and discussion

Various FGM plates and shells with different geometry and material properties are here investigated in order to analyze the effects of discarding and including the transverse normal strain ϵ_{zz}:

- one-layered FGM plates and shells with elastic properties varying along the thickness direction z by a polynomial law, as proposed by Zenkour [6];
- one-layered FGM plates with elastic properties varying in z by an exponential-law, as given by Kashtalyan [4];
- sandwich plates and shells with an FGM core and two isotropic faces, where the FGM properties are those given by Zenkour [6].

In each case, transverse normal strain effects have been explicitly evaluated. Errors with respect to the three-dimensional solutions are given. For those problems in which the 3D solution is not available, the related quasi-3D results have been provided by

Table 1
FGM isotropic plate with polynomial material law [6]. Effect of transverse normal strain ϵ_{zz} for a bending problem.

	a/h	ϵ_{zz}	$\bar{\sigma}_{xx}(h/3)$			$\bar{u}_z(0)$		
			4	10	100	4	10	100
$\kappa = 1$	Ref. [27]	$\neq 0$	0.6221	1.5064	14.969	0.7171	0.5875	0.5625
	CLT	0	0.8060	2.0150	20.150	0.5623	0.5623	0.5623
	FSDT($\chi = 5/6$)	0	0.8060	2.0150	20.150	0.7291	0.5889	0.5625
	GSDT [6]	0	–	1.4894	–	–	0.5889	–
	$N = 1$	$\neq 0$	0.8452	2.0311	20.151	0.6985	0.5844	0.5625
	Err%		(35.86)	(34.83)	(34.62)	(2.59)	(0.53)	(0)
	$N = 1$	0	0.8059	2.0150	20.150	0.7013	0.5845	0.5625
	Err%		(29.54)	(33.76)	(34.61)	(2.20)	(0.51)	(0)
	$N = 4$	$\neq 0$	0.6221	1.5064	14.969	0.7171	0.5875	0.5625
	Err%		(0)	(0)	(0)	(0)	(0)	(0)
	$N = 4$	0	0.7856	2.0068	20.149	0.7289	0.5890	0.5625
	Err%		(26.28)	(33.22)	(34.60)	(1.64)	(0.25)	(0)
$\kappa = 4$	Ref. [27]	$\neq 0$	0.4877	1.1971	11.923	1.1585	0.8821	0.8286
	CLT	0	0.6420	1.6049	16.049	0.8281	0.8281	0.8281
	FSDT($\chi = 5/6$)	0	0.6420	1.6049	16.049	1.1125	0.8736	0.8286
	GSDT [6]	0	–	1.1783	–	–	0.8651	–
	$N = 1$	$\neq 0$	0.6816	1.6213	16.051	1.0593	0.8659	0.8285
	Err%		(39.76)	(35.43)	(34.62)	(8.56)	(1.84)	(0.01)
	$N = 1$	0	0.6420	1.6049	16.049	1.0651	0.8660	0.8285
	Err%		(31.64)	(34.06)	(34.60)	(8.06)	(1.82)	(0.01)
	$N = 2$	$\neq 0$	0.4950	1.1998	11.923	1.1032	0.8729	0.8286
	$N = 2$	0	0.6336	1.6014	16.049	1.0947	0.8710	0.8286
	$N = 3$	$\neq 0$	0.4694	1.1895	11.922	1.1562	0.8816	0.8286
	$N = 3$	0	0.5946	1.5856	16.047	1.1645	0.8823	0.8286
	$N = 4$	$\neq 0$	0.4877	1.1971	11.923	1.1585	0.8821	0.8286
	Err%		(0)	(0)	(0)	(0)	(0)	(0)
	$N = 4$	0	0.5986	1.5874	16.047	1.1673	0.8828	0.8286
	Err%		(22.74)	(32.60)	(34.59)	(0.76)	(0.08)	(0)
κ=10	Ref. [27]	$\neq 0$	0.3695	0.8965	8.9077	1.3745	1.0072	0.9361
	CLT	0	0.4796	1.1990	11.990	0.9354	0.9354	0.9354
	FSDT($\chi = 5/6$)	0	0.4796	1.1990	11.990	1.3178	0.9966	0.9360
	GSDT [6]	0	–	0.8775	–	–	1.0089	–
	$N = 1$	$\neq 0$	0.5117	1.2124	11.992	1.2475	0.9862	0.9359
	Err%		(38.48)	(26.05)	(34.62)	(9.24)	(2.08)	(0.0002)
	$N = 1$	0	0.4796	1.1990	11.990	1.2541	0.9864	0.9359
	Err%		(29.79)	(33.74)	(34.60)	(8.76)	(2.06)	(0.0002)
	$N = 4$	$\neq 0$	0.1478	0.8965	8.9077	1.3745	1.0072	0.9361
	Err%		(0)	(0)	(0)	(0)	(0)	(0)
	$N = 4$	0	0.4345	1.1807	11.989	1.3925	1.0090	0.9361
	Err%		(17.59)	(31.70)	(34.59)	(1.31)	(0.001)	(0)

Table 2
FGM isotropic plate with exponential material law [4]. Effect of transverse normal strain ϵ_{zz} for a bending problem. Exponential γ equal to 0.1.

a/h	ϵ_{zz}	$\bar{u}_x(-\frac{h}{4})$	$\bar{u}_x \times 10^{-2}(-\frac{h}{4})$	$\bar{u}_x \times 10^{-4}(-\frac{h}{4})$	$\bar{u}_z(0)$	$\bar{u}_z \times 10_{-3}(0)$	$\bar{u}_z \times 10_{-6}(0)$
		3	20	100	3	20	100
3D[4]	0	n.d.	n.d.	n.d.	1.4146	n.d	n.d.
Ref. [27]	≠0	0.2453	0.7356	0.9198	1.4145	1.8363	1.1340
CLT	0	0.2483	0.7358	0.9197	0.9180	1.8133	1.1333
FSDT(χ = 5/6)	0	0.2483	0.7358	0.9197	1.4929	1.8388	1.1339
N = 1	≠0	0.2749	0.7377	0.9198	1.3955	1.8346	1.1338
Err%		(12.07)	(0.28)	(0)	(1.34)	(0.10)	(0.15)
N = 1	0	0.2483	0.7358	0.9197	1.3971	1.8345	1.1338
Err%		(1.22)	(0.03)	(0)	(1.23)	(0.10)	(0)
N = 2	≠0	0.2684	0.7370	0.9198	1.3480	1.8330	1.1338
N = 2	0	0.2486	0.7358	0.9197	1.3972	1.8346	1.1338
N = 3	≠0	0.2458	0.7356	0.9197	1.4167	1.8361	1.1339
N = 3	0	0.2274	0.7343	0.9197	1.4889	1.8388	1.1339
N = 4	≠0	0.2453	0.7356	0.9198	1.4145	1.8363	1.1340
Err%		(0)	(0)	(0)	(0)	(0)	(0)
N = 4	0	0.2273	0.7343	0.9197	1.4889	1.8388	1.1339
Err%		(7.34)	(0.18)	(0.01)	(5.26)	(0.14)	(0.07)

Table 3
Sandwich plate embedding an FGM core with polynomial material law [6]. Effect of transverse normal strain ϵ_{zz} for a bending problem.

	a/h	ϵ_{zz}	$\bar{\sigma}_{xz}(h/6)$			$\bar{u}_z(0)$		
			4	10	100	4	10	100
κ = 1	Ref. [29]	≠0	0.2613	0.2605	0.2603	0.7628	0.6324	0.6072
	CLT	0	0.0000	0.0000	0.0000	0.6070	0.6070	0.6070
	FSDT(χ = 5/6)	0	0.2458	0.2458	0.2458	0.7738	0.6337	0.6073
	N = 1	≠0	0.2059	0.2050	0.2048	0.7429	0.6292	0.6072
	Err%		(21.20)	(21.30)	(21.32)	(2.61)	(0.51)	(0)
	N = 1	0	0.2048	0.2048	0.2048	0.7429	0.6292	0.6072
	Err%		(21.62)	(21.38)	(21.32)	(2.61)	(0.51)	(0)
	N = 4	≠0	0.2604	0.2594	0.2593	0.7628	0.6324	0.6072
	Err%		(0.34)	(0.42)	(0.38)	(0)	(0)	(0)
	N = 4	0	0.2596	0.2593	0.2593	0.7735	0.6337	0.6072
	Err%		(0.65)	(0.46)	(0.38)	(1.40)	(0.20)	(0)
κ = 4	Ref. [29]	≠0	0.2429	0.2431	0.2432	1.0934	0.8321	0.7797
	CLT	0	0.0000	0.0000	0.0000	0.7792	0.7792	0.7792
	FSDT(χ = 5/6)	0	0.1877	0.1877	0.1877	1.0285	0.8191	0.7796
	N = 1	≠0	0.1561	0.1564	0.1564	0.9814	0.8123	0.7795
	Err%		(35.73)	(35.66)	(35.69)	(10.24)	(2.38)	(0.02)
	N = 1	0	0.1564	0.1564	0.1564	0.9869	0.8124	0.7795
	Err%		(35.61)	(35.66)	(35.69)	(9.74)	(2.37)	(0.02)
	N = 2	≠0	0.1719	0.1721	0.1722	1.0383	0.8227	0.7796
	N = 2	0	0.1598	0.1599	0.1599	1.0271	0.8192	0.7796
	N = 3	≠0	0.2575	0.2589	0.2592	1.0872	0.8308	0.7797
	N = 3	0	0.2570	0.2588	0.2592	1.0916	0.8296	0.7797
	N = 4	≠0	0.2400	0.2398	0.2398	1.0930	0.8307	0.7797
	Err%		(1.20)	(1.35)	(1.40)	(0.04)	(0.17)	(0)
	N = 4	0	0.2400	0.2398	0.2398	1.0977	0.8308	0.7797
	Err%		(1.20)	(1.35)	(1.40)	(0.39)	(0.16)	(0)
κ = 10	Ref. [29]	≠0	0.2150	0.2174	0.2179	1.2232	0.8753	0.8077
	CLT	0	0.0000	0.0000	0.0000	0.8070	0.8070	0.8070
	FSDT(χ = 5/6)	0	0.1234	0.1234	0.1234	1.1109	0.8556	0.8075
	N = 1	≠0	0.1028	0.1028	0.1029	1.0537	0.8473	0.8074
	Err%		(52.18)	(52.71)	(52.77)	(13.85)	(3.19)	(0.04)
	N = 1	0	0.1028	0.1028	0.1077	1.0602	0.8475	0.8074
	Err%		(52.18)	(52.71)	(52.80)	(13.32)	(3.18)	(0.04)
	N = 4	≠0	0.1932	0.1944	0.1946	1.2172	0.8740	0.8077
	Err%		(10.14)	(10.58)	(10.69)	(0.49)	(0.15)	(0)
	N = 4	0	0.1935	0.1944	0.1946	1.2240	0.8743	0.8077
	Err%		(10.00)	(10.58)	(10.69)	(0.06)	(0.11)	(0)

a discrete model with mathematical layers already developed in [27–30] to validate the refined and mixed models for FGM plates and shells. These discrete-layer approaches are however very expensive from a computational point of view. CLT and FSDT results given in Tables 1–5 are obtained from CUF models as particular cases by a typical penalty technique (the same MUL2 in-house academic software introduced in Section 1 has been used).

Attention has been restricted to simply supported FGM multilayered plate/shell geometries loaded by a bi-sinusoidal pressure, where m and n indicate the number of waves along the α and β directions, respectively. Closed form solution of the proposed governing differential equations have been derived according to the solution strategies (based on Navier type-solutions) described in the previous authors' papers [26,27].

5.1. One-layered FGM plate

In the case of one-layered FGM plates, two different assessments are provided: an isotropic FGM plate with a polynomial material law, as given by Zenkour [6], and an isotropic FGM plate with an exponential material law, as given by Kashtalyan [4].

First, a square plate with $a = b = 1$ m is considered. It is simply supported with a bi-sinusoidal transverse mechanical load, of amplitude $\bar{p}_z = 1$ Pa and $m = m = 1$, applied to its top. The considered thickness ratios a/h are 4, 10 and 100, which means thickness h equals 0.25 m, 0.1 m and 0.01 m, respectively. The plate is graded from aluminum (bottom) to alumina (top). The following functional relationship is considered for Young's modulus $E(z)$ in the thickness direction z [6]:

$$E(z) = E_m + (E_c - E_m)\left(\frac{2z+h}{2h}\right)^{\kappa}, \quad -\frac{h}{2} \leqslant z \leqslant \frac{h}{2}, \tag{10}$$

where $E_m = 70$ GPa and $E_c = 380$ GPa are the corresponding properties of the metal and ceramic, respectively; κ is the volume fraction exponent which is a positive number. The Poisson ratio is considered constant and equal to 0.3. The results, in this case, are given in terms of the following non-dimensional parameters:

$$\bar{u}_z = \frac{10h^3 E_c}{a^4 \bar{p}_z} u_z, \quad \bar{\sigma}_{xx} = \frac{h}{a\bar{p}_z}\sigma_{xx}, \quad \bar{\sigma}_{xz} = \frac{h}{a\bar{p}_z}\sigma_{xz}, \quad \bar{\sigma}_{zz} = \sigma_{zz}.$$

The results for various theories are given in Table 1. The effect of ϵ_{zz} is evident for each proposed plate theory. Three values of the FGM exponent κ are treated. The reference solution is obtained by means of a discrete model, as described in [27]. GSDT is the Generalized Shear Deformation Theory, as proposed by Zenkour [6], FSDT is the first-order shear deformation theory obtained with CUF [34] with a shear correction factor $\chi = 5/6$. The $N = 1(\epsilon_{zz} = 0)$ theory is the FSDT theory with $\chi = 1$.

The following remarks can be made:

- results related to theories that discard transverse normal strains merge with those that retain transverse normal deformations; this happens for any order of expansion as well as for any FGM exponent κ; however, the error is almost zero for thin plates in the case of displacement evaluation;

Table 4
FGM isotropic shell with polynomial material law [6]. Effect of transverse normal strain ϵ_{zz} for a bending problem.

	R_x/h	ϵ_{zz}	$u_z \times 10^{-11}(0)$			
			4	10	100	1000
$\kappa = 1$	Ref. [30]	$\neq 0$	0.0131	0.1696	52.745	4201.4
	CLT	0	0.0042	0.0611	40.445	4201.6
	FSDT($\chi = 5/6$)	0	0.0649	0.2049	52.863	4201.7
	$N = 1$	$\neq 0$	0.0281	0.1619	52.978	4419.9
	Err%		(55.55)	(4.54)	(0.44)	(4.94)
	$N = 1$	0	0.0549	0.1810	52.680	4201.7
	Err%		(>100)	(6.72)	(0.12)	(0.007)
	$N = 2$	$\neq 0$	0.0063	0.1595	52.653	4201.4
	$N = 2$	0	0.0557	0.1858	52.728	4201.7
	$N = 3$	$\neq 0$	0.0082	0.1690	52.743	4201.4
	$N = 3$	0	0.0596	0.2016	52.866	4201.7
	$N = 4$	$\neq 0$	0.0027	0.1671	52.745	4201.4
	Err%		(83.33)	(1.47)	(0)	(0)
	$N = 4$	0	0.0598	0.2016	52.867	4201.7
	Err%		(>100)	(18.86)	(0.23)	(0.007)
$\kappa = 5$	Ref. [30]	$\neq 0$	0.0227	0.3416	82.643	7648.6
	CLT	0	0.0064	0.0929	80.185	7648.7
	FSDT($\chi = 5/6$)	0	0.1178	0.3582	82.296	7648.9
	$N = 1$	$\neq 0$	0.0480	0.2751	82.339	8039.7
	Err%		(>100)	(19.46)	(0.37)	(5.11)
	$N = 1$	0	0.993	0.3141	81.945	7648.9
	Err%		(>100)	(8.05)	(0.84)	(0.003)
	$N = 2$	$\neq 0$	0.0216	0.3039	82.151	7648.6
	$N = 2$	0	0.1031	0.3343	82.153	7648.9
	$N = 3$	$\neq 0$	0.0206	0.3433	82.626	7648.6
	$N = 3$	0	0.1187	0.3995	82.753	7649.0
	$N = 4$	$\neq 0$	-0.0011	0.3370	82.642	7648.6
	Err%		(95.15)	(1.35)	(0)	(0)
	$N = 4$	0	0.1193	0.3996	82.769	7649.0
	Err%		(>100)	(16.98)	(0.15)	(0.004)
$\kappa = 10$	Ref. [30]	$\neq 0$	0.0225	0.4054	92.014	9373.1
	CLT	0	0.0070	0.1018	88.974	9373.3
	FSDT($\chi = 5/6$)	0	0.1461	0.4316	91.648	9373.6
	$N = 1$	$\neq 0$	0.0705	0.3392	91.580	9846.7
	Err%		(>100)	(16.33)	(0.47)	(4.81)
	$N = 1$	0	0.1230	0.3768	91.203	9373.5
	Err%		(>100)	(7.05)	(0.88)	(0.004)
	$N = 2$	$\neq 0$	0.0315	0.3501	91.302	9373.0
	$N = 2$	0	0.1256	0.3888	91.321	9373.6
	$N = 3$	$\neq 0$	0.0316	0.4118	92.010	9373.1
	$N = 3$	0	0.1478	0.4810	92.187	9373.7
	$N = 4$	$\neq 0$	-0.0099	0.3980	92.012	9373.1
	Err%		(>100)	(1.82)	(0)	(0)
	$N = 4$	0	0.1497	0.4823	92.191	9373.7
	Err%		(>100)	(18.97)	(0.19)	(5.68)

Table 5
Sandwich shell embedding an FGM core with polynomial material law [6]. Effect of transverse normal strain ϵ_{zz} for a bending problem.

	R_x/h	ϵ_{zz}	$u_z \times 10^{-11}(0)$			
			4	10	100	1000
$\kappa = 1$	Ref. [30]	$\neq 0$	0.0175	0.1748	56.393	4224.0
	CLT	0	0.0046	0.0661	55.428	4223.3
	FSDT($\chi = 5/6$)	0	0.0659	0.2099	56.530	4224.5
	$N = 1$	$\neq 0$	0.0242	0.1648	56.351	4445.1
	Err%		(38.28)	(5.72)	(0.07)	(4.97)
	$N = 1$	0	0.0557	0.1860	56.699	4224.5
	Err%		(>100)	(6.41)	(0.54)	(0.01)
	$N = 2$	$\neq 0$	0.0049	0.1660	56.347	4224.2
	$N = 2$	0	0.0569	0.1928	56.420	4224.5
	$N = 3$	$\neq 0$	0.0061	0.1734	56.417	4224.3
	$N = 3$	0	0.0604	0.2064	56.533	4224.5
	$N = 4$	$\neq 0$	0.0019	0.1721	56.417	4224.3
	Err%		(89.14)	(1.54)	(0.04)	(0)
	$N = 4$	0	0.0608	0.2065	56.534	4224.5
	Err%		(>100)	(18.13)	(0.25)	(0.01)
$\kappa = 5$	Ref. [30]	$\neq 0$	0.0275	0.3123	75.947	6581.9
	CLT	0	0.0061	0.0864	73.651	6578.3
	FSDT($\chi = 5/6$)	0	0.1020	0.3129	75.437	6582.7
	$N = 1$	$\neq 0$	0.0345	0.2387	75.540	6921.4
	Err%		(25.45)	(23.56)	(0.53)	(4.90)
	$N = 1$	0	0.0860	0.2753	75.141	6582.7
	Err%		(>100)	(11.85)	(1.06)	(0.01)
	$N = 2$	$\neq 0$	0.0168	0.2799	75.463	6582.5
	$N = 2$	0	0.0914	0.3042	75.438	6582.7
	$N = 3$	$\neq 0$	0.0151	0.3154	75.898	6582.5
	$N = 3$	0	0.1060	0.3648	75.988	6582.7
	$N = 4$	$\neq 0$	0.0008	0.3125	75.941	6582.5
	Err%		(>100)	(0.06)	(0.007)	(0)
	$N = 4$	0	0.1063	0.3658	76.031	6582.7
	Err%		(>100)	(17.13)	(0.11)	(0.01)
$\kappa = 10$	Ref. [30]	$\neq 0$	0.0262	0.3622	79.092	7506.7
	CLT	0	0.0062	0.0884	76.235	7505.5
	FSDT($\chi = 5/6$)	0	0.1169	0.3496	78.346	7507.6
	$N = 1$	$\neq 0$	0.0441	0.2658	78.350	7889.8
	Err%		(56.87)	(26.61)	(0.94)	(5.10)
	$N = 1$	0	0.0985	0.3062	77.982	7507.6
	Err%		(>100)	(15.46)	(1.40)	(0.01)
	$N = 2$	$\neq 0$	0.0237	0.3101	78.305	7507.4
	$N = 2$	0	0.1040	0.3339	78.259	7507.6
	$N = 3$	$\neq 0$	0.0217	0.3706	79.038	7507.5
	$N = 3$	0	0.1272	0.4290	79.135	7507.7
	$N = 4$	$\neq 0$	-0.0037	0.3628	79.040	7507.5
	Err%		(>100)	(0.16)	(0.06)	(0.0001)
	$N = 4$	0	0.1286	0.4291	79.137	7507.7
	Err%		(>100)	(18.47)	(0.06)	(0.01)

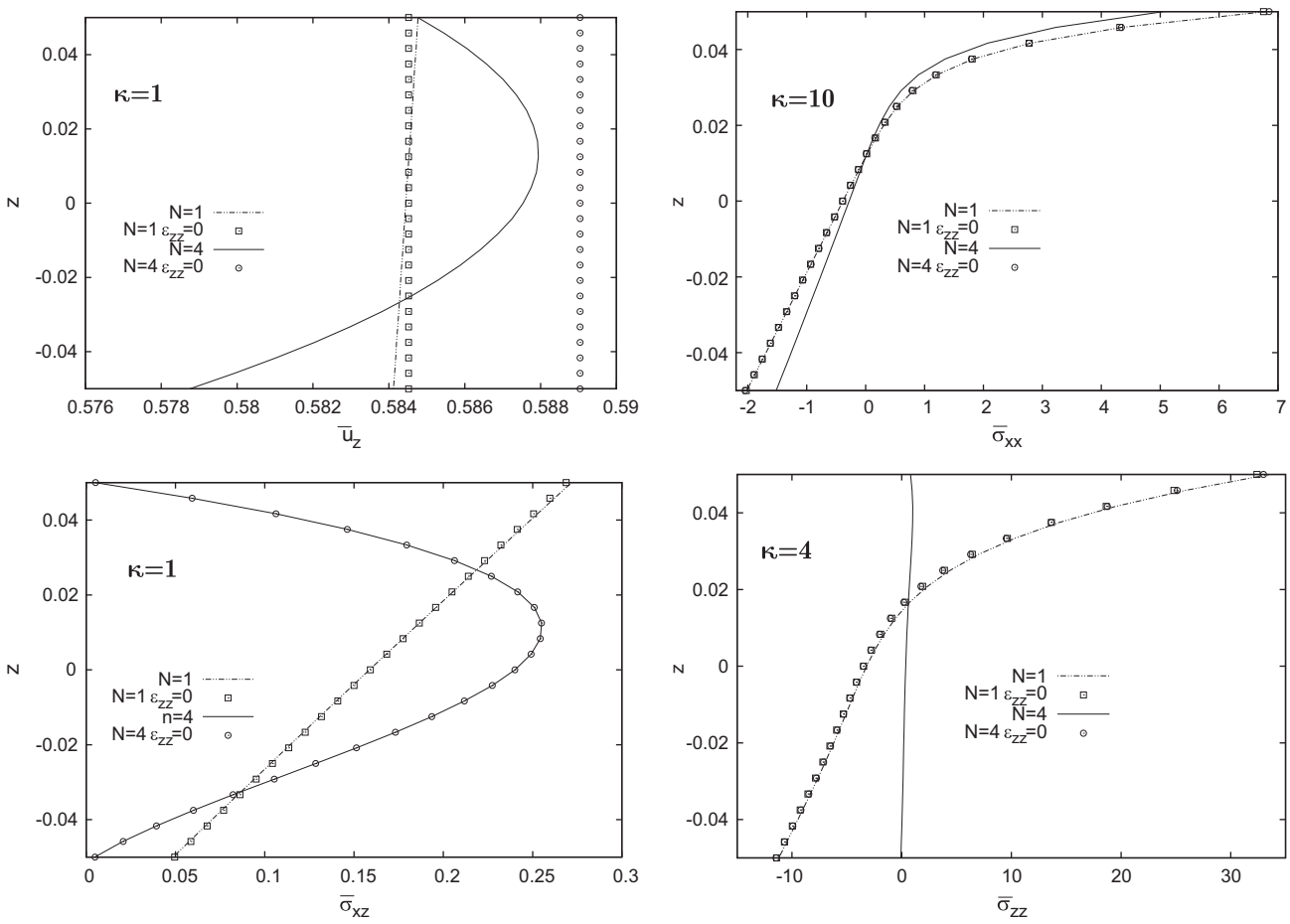

Fig. 3. FGM isotropic plate with polynomial material law [6], thickness ratio $a/h = 10$. Displacement and stresses through the thickness direction z for different values of κ.

- as stated in Koiter's recommendation, the transverse strain error is almost independent of the order of the expansion N used by the implemented higher-order theory: there is no sense in increasing (refining) the order of the expansion of the in-plane displacements u_x and u_y, without including transverse normal strains;
- the ϵ_{zz} effect is much more significant in the stress evaluation with respect to the transverse displacement components; in the stress evaluation, the error is independent of the considered thickness ratio;
- the ϵ_{zz} effect is slightly dependent on exponent κ.

The distributions of stress and displacement components through the plate thickness direction z are given in Fig. 3 in the case of a thick plate ($a/h = 10$). Linear and the fourth-order theories are compared. It is evident that the transverse normal strain effects depend on the position in the z direction: for particular values of z, the error is larger, and this aspect is fundamental for a better understanding of Table 1. In Fig. 3 the plate is thick, so in the first picture the hypothesis of constant transverse displacement is completely wrong and a linear expansion in the thickness direction for this displacement component is also inappropriate. The considered FGM material uses isotropic constitutive equations and for this reason in the in-plane stress σ_{xx} the contribution of in-plane strains is more important than that of the transverse normal strain, even if this last one gives a perceptible difference (see second picture). In the third picture the transverse shear stress σ_{xz} depends on the strain $\gamma_{xz} = \frac{\partial w}{\partial x} + \frac{\partial u}{\partial z}$, and this means that higher orders of expansion in the thickness direction are requested for the in-plane displacement components and not for the transverse displacement component. Finally, the last picture demonstrates as for the transverse normal stress σ_{zz} the contribution of the transverse normal strain ϵ_{zz} is fundamental.

The second case is a simply supported FGM plate with an exponential material law, as indicated in [4] by Kashtalyan. A transverse bi-sinusoidal pressure ($m = n = 1$) of amplitude $\bar{p}_z = 1$ Pa is applied to its top. The square plate ($a = b$) has dimensions 3 m, 20 m and 100 m, and thickness h equal to 1 m, which means thickness ratios a/h equal to 3, 20 and 100, respectively. According to [4], the shear modulus $G(z)$ is assumed to vary exponentially through the thickness z (the Poisson ratio is considered to be constant) according to:

$$G(z) = G_1 e^{\gamma(z/h-1)}, \quad G_1 = \frac{E_1}{2(1+\nu)}, \quad 0 \leqslant z \leqslant h, \tag{11}$$

where $E_1 = 73$ GPa and $\nu = 0.3$. The exponential γ is equal to 0.1, and $\gamma = 0$ means homogeneous material.

The in-plane displacement $\bar{u}_x = u_x \frac{G_1}{\bar{p}_z h}$ in $z = -\frac{h}{4}$ and the out-of-plane displacement $\bar{u}_z = u_z \frac{G_1}{\bar{p}_z h}$ in $z = 0$ are given in Table 2. The 3D solution is given by Kashtalyan [4] for $a/h = 3$, while for the other thickness ratios, a quasi-3D solution is provided, as described in [27]. Higher-order theories ($N = 4$) which neglect the transverse normal strain give a larger error than 5% for both in-plane and out-of-plane displacements; the error disappears for thin plates ($a/h = 100$). Fig. 4 shows the variation along thickness z for displacements and stresses (σ_{xx}, σ_{xz} and σ_{zz}). The comments made for the previous plate case are confirmed for this different thickness law: the employed constitutive equations are also isotropic in this case.

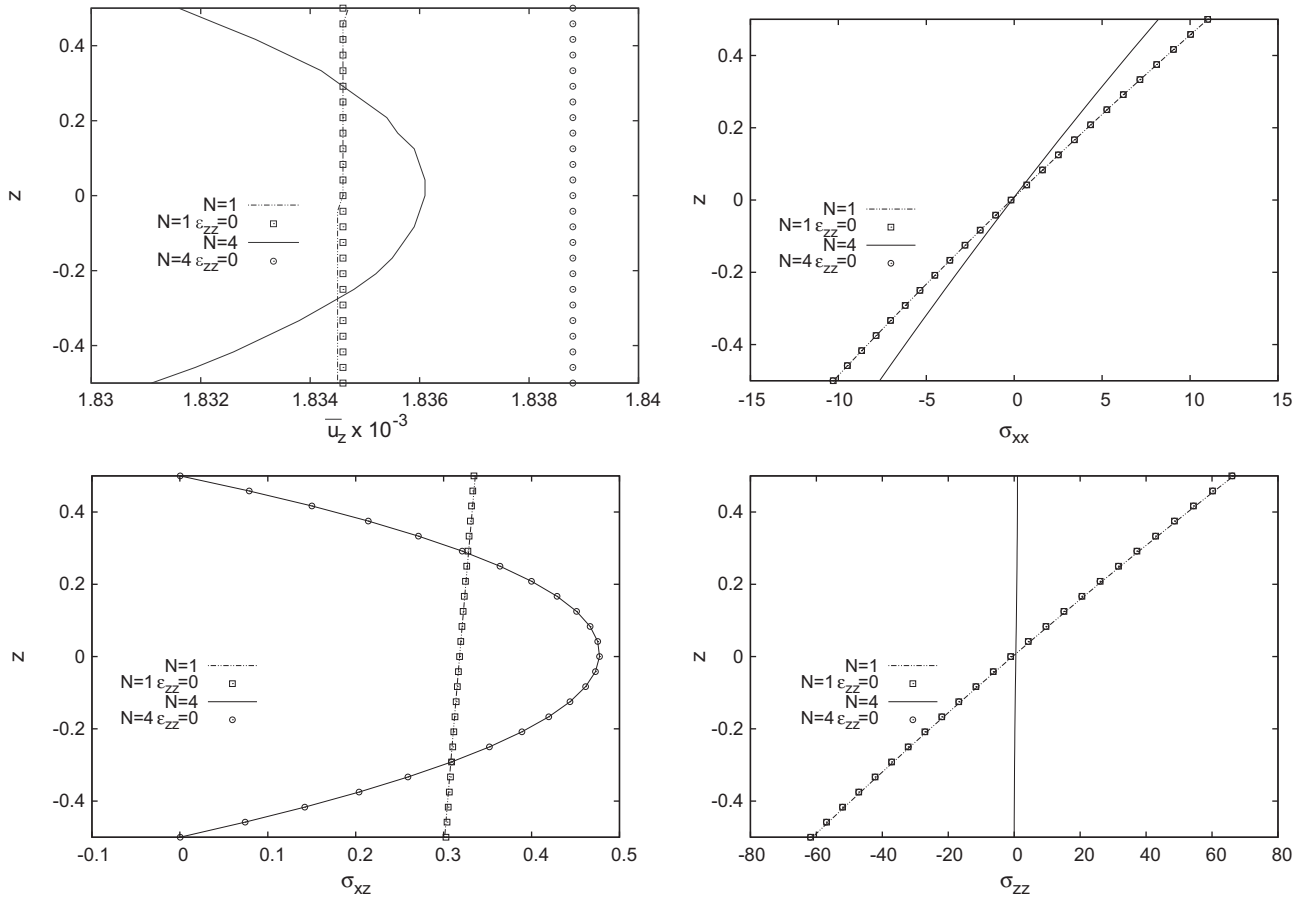

Fig. 4. FGM isotropic plate with exponential material law [4], thickness ratio $a/h = 20$. Displacement and stresses through the thickness direction z for $\gamma = 0.1$.

In Fig. 4, it is clear how HOTs discarding ϵ_{zz} have a larger error near the top and bottom than in the middle of the plate. This fact is very useful to discuss some results in Table 2.

5.2. Sandwich plate with an FGM core

A simply supported square sandwich plate ($a = b = 1$ m) is considered, with a total thickness h equal to 0.25 m, 0.1 m, 0.01 m, which means a thickness ratio a/h equal to 4, 10, 100, respectively. The bi-sinusoidal load is the same as the one-layered FGM cases. The two external faces are in aluminium at the bottom ($E_m = E_1 = 70$ GPa and $h_1 = 0.1h$), and in alumina at the top ($E_c = E_3 = 380$ GPa and $h_3 = 0.1h$). The internal core is in FGM ($h_2 = 0.8h$) according to the polynomial law in Eq. (10). The Poisson ratio is constant for each layer and is equal to 0.3. Several thickness ratios and exponential κ in Eq. (10), are investigated in Table 3, in terms of transverse displacement $\bar{u}_z = u_z \frac{10E_c h^3}{a^4 \bar{p}_z}$ and transverse shear stress $\bar{\sigma}_{xz} = \sigma_{xz} \frac{h}{a\bar{p}_z}$. The reference solution is a quasi-3D one, as proposed in [29]. For thickness ratio $a/h = 10$ and exponential $\kappa = 4$, displacements and stresses through thickness z are given in Fig. 5 ($\bar{\sigma}_{xx} = \sigma_{xx} \frac{h}{a\bar{p}_z}$, $\bar{\sigma}_{zz} = \sigma_{zz}$). The explanation of these pictures is the same given in the previous section for the one-layered FGM plates, even if the differences for the multilayered plate are larger because of the bigger transverse anisotropy. Further comments, with respect to those given in Section 5.1 for one-layered plates, can be made:

- in the case of transverse shear stress evaluation, the error is larger with respect to the displacement evaluation and it is not reduced by increasing the thickness ratio; in this case, the use of layer wise theories is mandatory;
- for displacements, the error is smaller and a higher order theory ($N = 4$) including ϵ_{zz} is sufficient;
- in Table 3, the values of displacements and stresses seem very close for both models including and discarding ϵ_{zz}, but it is clear from Fig. 5 that such a difference is much larger in some other points along the thickness.

5.3. One-layered FGM shell

The considered shell is an isotropic FGM with a polynomial material law [6] as previously given in Section 5.1. The bi-sinusoidal load is applied to the top (amplitude $\bar{p}_z = 1$ Pa and waves number $m = n = 1$). A simply supported Ren shell geometry is considered. The curvature radii are $R_\alpha = 10$ m in the α direction and $R_\beta = \infty$ in the β direction. The dimension b is equal to 1 m, the dimension in the α direction is $a = \frac{\pi}{3} R_\alpha = 10.471975513\ m$. The considered thickness h is 2.5 m, 1 m, 0.1 m and 0.01 m, which means a thickness ratio R_α/h equal to 4, 10, 100 and 1000, respectively. The transverse displacement u_z in $z = 0$ is given in Table 4 for several thickness ratios R_α/h and exponential κ. The reference quasi-3D solution for a shell geometry is calculated as described in [30] by means of a discret model. Only displacement u_z and transverse shear normal stress σ_{zz} along the z direction of the considered shell are given in Fig. 6 (for $R_\alpha/h = 10$ and $\kappa = 5$) because the introduction of the curvatures does not modify the conclusions already given for the correspondent plate cases. However, larger values of error in percentage are observed. It is clearly indicated in Fig. 6, for both displacements and stresses, how larger errors appear near the top and bottom of the structure when the ϵ_{zz} effect is discarded.

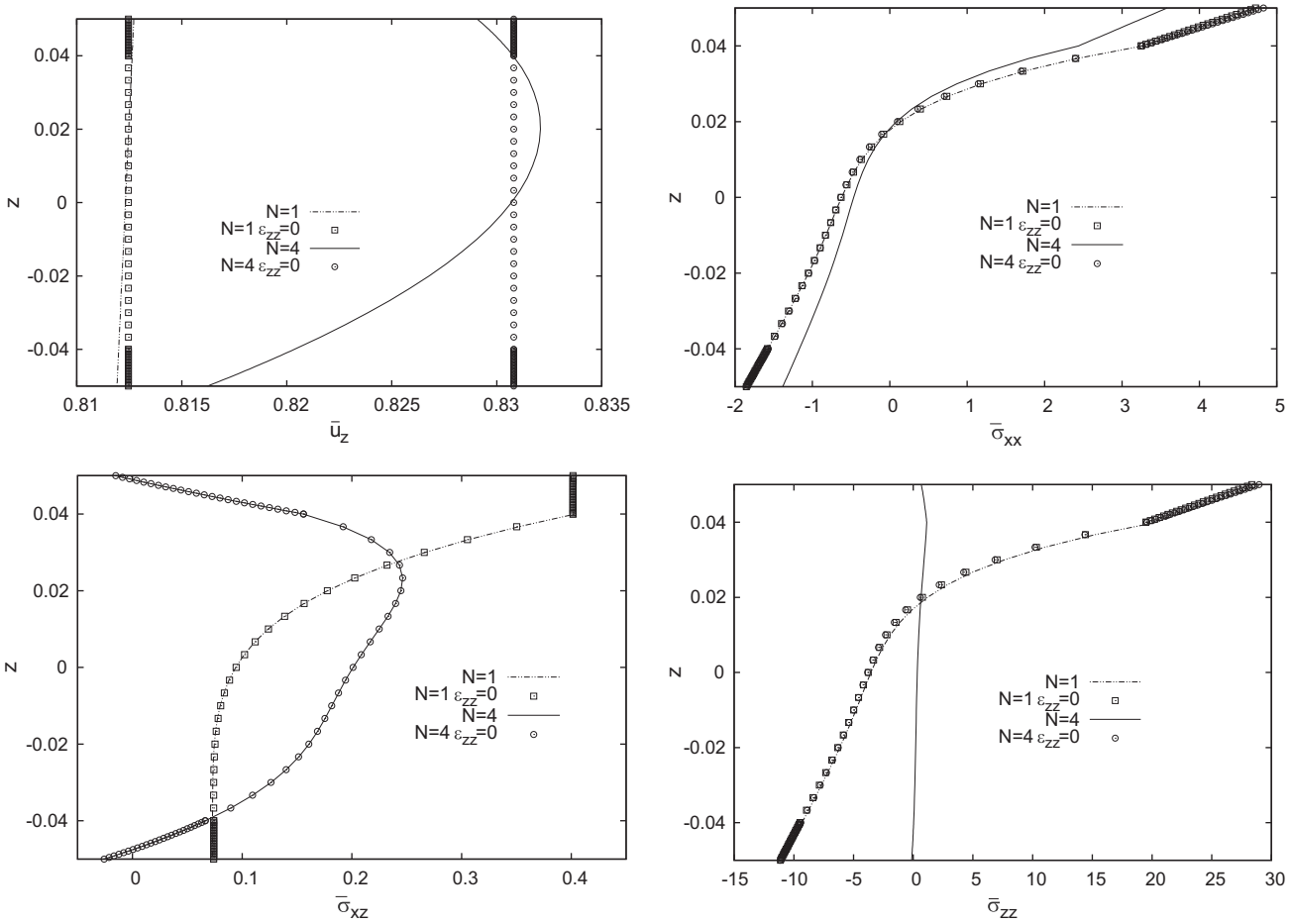

Fig. 5. Sandwich plate embedding an FGM core with polynomial material law [6], thickness ratio $a/h = 10$. Displacement and stresses through the thickness direction z for $\kappa = 4$.

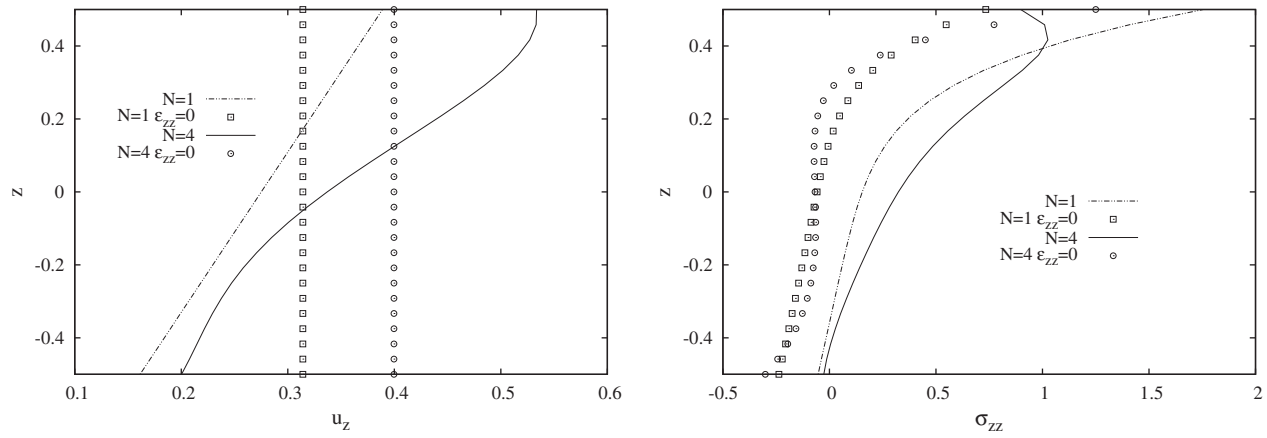

Fig. 6. FGM isotropic shell with polynomial material law [6], thickness ratio $R_\alpha/h = 10$. Displacement and transverse normal stress through the thickness direction z for $\kappa = 5$.

5.4. Sandwich shell with an FGM core

The considered sandwich shell has the same geometrical properties as the one-layered shell presented in Section 5.3; in this case the total thickness h is 2.5 m, 1 m, 0.1 m and 0.01 m. The loading conditions have already been discussed in the previous sections. Like the plate geometry in Section 5.2, the two external faces are in ceramic (top) and metallic (bottom); the core is in FGM, according to Zenkour's law in Eq. (10). The core has a thickness $h_2 = 0.8$ h and the two faces have $h_1 = h_3 = 0.1$ h. The transverse displacement u_z in $z = 0$ is given in Table 5 for several thickness ratios R_α/h and different exponential κ for Zenkour's law. A quasi-3D solution, like the one obtained in [30], is used as a reference. Fig. 7 gives the transverse displacement and the transverse normal stress through z for $R_\alpha/h = 10$ and $\kappa = 5$. The effects of transverse normal strain ϵ_{zz} are the same as those observed for the correspondent plate case. The curvature does not play a new role with respect to the sandwich plate. The importance of the ϵ_{zz} effect is clearly demonstrated

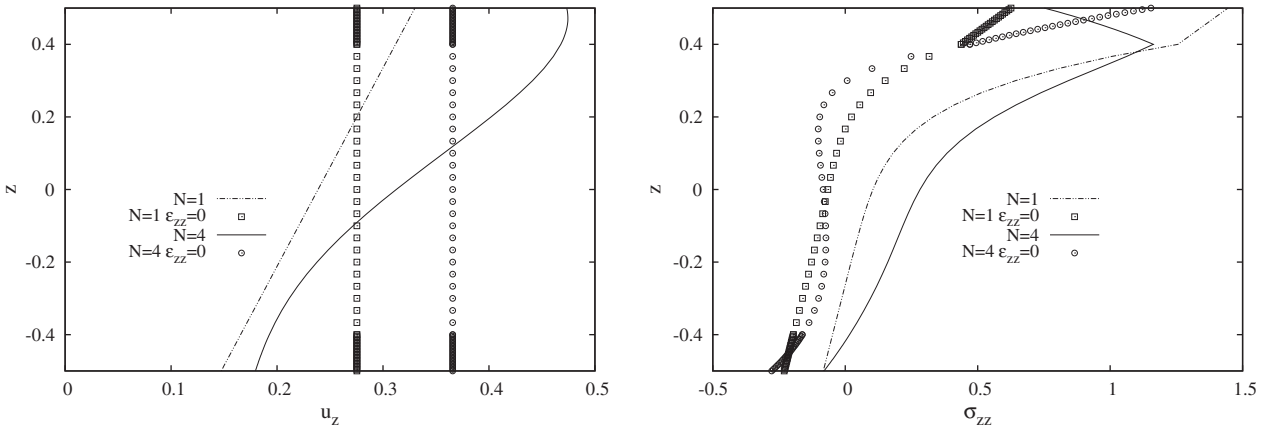

Fig. 7. Sandwich shell embedding an FGM core with polynomial material law [6], thickness ratio $R_x/h = 10$. Displacement and transverse normal stress through the thickness direction z for $\kappa = 5$.

in Table 5 for thick shells, and it seems less important for thin shells. However it is shown in Fig. 7 that this fact is not valid for each value of the thickness coordinate z.

6. Concluding remarks

The paper proposes an exhaustive investigation of the transverse normal strain effects in classical and higher-order two-dimensional theories for one-layered and multilayered plates and shells embedding functionally graded material (FGM) layers. The proposed higher-order theories (order of expansion N in the thickness direction for the three displacement components from 1 to 4) have been implemented by referring to Carrera's Unified Formulation (CUF). Classical theories, such as Classical Lamination Theory (CLT) and First order Shear deformation Theory (FSDT), have been obtained as particular cases of the $N = 1$ CUF higher-order model. The transverse normal strain effects in higher-order theories have been investigated by imposing a constant transverse displacement and an order of expansion $N = 1, \ldots, 4$ for the two in-plane displacement components.

From the analysis of the results, the following main conclusions can be drawn:

- Koiter's recommendation appears relevant in FGM structures analysis, that is, an increase in the order of expansion for in-plane displacements can result meaningless if the thickness stretching is discarded in the plate/shell theories (constant transverse displacement);
- ϵ_{zz} effect plays a significant role in thick and moderately thick plates and shells;
- ϵ_{zz} effect depends on the considered FGM material (thickness law), on the number of layers and their sequence in the thickness direction;
- ϵ_{zz} effect depends on the transverse anisotropy of the considered structure and on the investigated variable;
- ϵ_{zz} effect cannot be neglected in the case of sandwich plates and shells even though the considered structures are thin; in these cases the use of layer wise models could result sometime mandatory;
- the conclusions obtained for plates are the same remarked for shells, which means that the curvature does not introduce further effects.

Future works would consider multifield problems and in particular the thermo-mechanical FGM plate/shell analysis will be investigated.

Acknowledgement

The authors acknowledge the Regione Piemonte for supporting the present research work by means of the regional STEPS project.

References

[1] Koizumi M. The concept of FGM. Ceramic transactions. Funct Grad Mater 1993;34:3–10.
[2] Koizumi M. FGM activities in Japan. Composites: Part B 1997;28:1–4.
[3] Birman B, Byrd LW. Modeling and analysis of functionally graded materials and structures. Appl Mech Rev 2007;60:195–216.
[4] Kashtalyan M. Three-dimensional elasticity solution for bending of functionally graded rectangular plates. Euro J Mech A/Solids 2004;23:853–64.
[5] Kashtalyan M, Menshykova M. Three-dimensional elasticity solution for sandwich panels with a functionally graded core. Compos Struct 2008;87:36–43.
[6] Zenkour AM. Generalized shear deformation theory for bending analysis of functionally graded plates. Appl Math Modell 2006;30:67–84.
[7] Batra RC, Jin J. Natural frequencies of a functionally graded anisotropic rectangular plate. J Sound Vib 2005;282:509–16.
[8] Qian LF, Batra RC, Chen LM. Static and dynamic deformations of thick functionally graded elastic plates by using higher-order shear and normal deformable plate theory and meshless local Petrov–Galerkin method. Composites: Part B 2004;35:685–97.
[9] Mori T, Tanaka K. Average stress in matrix and average elastic energy of materials with misfitting inclusions. Acta Metall 1973;21:571–4.
[10] Ramirez F, Heyliger PR, Pan E. Static analysis of functionally graded elastic anisotropic plates using a discrete layer approach. Composites: Part B 2006;37:10–20.
[11] Pan E. Exact solution for functionally graded anisotropic elastic composite laminates. J Compos Mater 2003;37:1903–20.
[12] Pagano NJ. Exact solutions for rectangular bidirectional composites and sandwich plates. J Compos Mater 1969;4:20–34.
[13] Pagano NJ. Exact solutions for composite laminates in cylindrical bending. J Compos Mater 1970;3:398–411.
[14] Vel SS, Batra RC. Three-dimensional exact solution for the vibration of functionally graded rectangular plates. J Sound Vib 2004;272:703–30.
[15] Vel SS, Batra RC. Three-dimensional analysis of transient thermal stresses in functionally graded plates. Int J Solids Struct 2002;40:7181–96.
[16] Ferreira AJM, Batra RC, Roque CMC, Qian LF, Martins PALS. Static analysis of functionally graded plates using third-order shear deformation theory and a meshless method. Compos Struct 2004;69:449–57.
[17] Chi SH, Chung YL. Mechanical behavior of functionally graded material plates under transverse load. Part I: analysis. Int J Solids Struct 2006;43:3657–74.
[18] Chi SH, Chung YL. Mechanical behavior of functionally graded material plates under transverse load. Part II: numerical results. Int J Solids Struct 2006;43:3675–91.
[19] Bayat M, Saleemb M, Sahari BB, Hamouda AMS, Mahdi E. Analysis of functionally graded rotating disks with variable thickness. Mech Res Commun 2008;35:283–309.
[20] Chiba R. Stochastic heat conduction analysis of a functionally graded annular disc with spatially random heat transfer coefficients. Appl Math Modell 2009;33:507–23.
[21] Estili M, Takagi K, Kawasaki A. Multiwalled carbon nanotubes as a unique agent to fabricate nanostructure-controlled functionally graded alumina ceramics. Scr Mater 2008;59:703–5.

[22] Haddadpour H, Mahmoudkhani S, Navazi HM. Supersonic flutter prediction of functionally graded cylindrical shells. Compos Struct 2008;83:391–8.
[23] Na KS, Kim JH. Optimization of volume fractions for functionally graded panels considering stress and critical temperature. Compos Struct 2009;89:509–16.
[24] Carrera E. Evaluation of layer-wise mixed theories for laminated plates analysis. AIAA J 1998;26:830–9.
[25] Carrera E. Developments, ideas and evaluations based upon Reissner's mixed variational theorem in the modeling of multilayered plates and shells. Appl Mech Rev 2001;54:301–29.
[26] Carrera E. Theories and finite elements for multilayered plates and shells: a unified compact formulation with numerical assessments and benchmarks. Arch Computat Meth Eng 2003;10:215–96.
[27] Carrera E, Brischetto S, Robaldo A. Variable kinematic model for the analysis of functionally graded material plates. AIAA J 2008;46:194–203.
[28] Brischetto S, Carrera, E. Advanced mixed theories for bending analysis of functionally graded plates, Computers and Structures, in press, available online on May.
[29] Brischetto S. Classical and mixed advanced models for sandwich plates embedding functionally graded cores. J Mech Mater Struct 2009;4:13–33.
[30] Brischetto S, Carrera E. Classical and mixed theories for bending analysis of functionally graded materials shells. Proceedings of APCOM'07 in conjunction with EPMESC XI, Kyoto, Japan; 2007.
[31] Koiter WT. A consistent first approximation in the general theory of thin elastic shells. In: Proceedings of first symposium on the theory of thin elastic shells. North-Holland, Amsterdam; 1959.
[32] Carrera E. Transverse normal stress effects in multilayered plates. J Appl Mech 1999;66:1004–12.
[33] Carrera E. A study of transverse normal stress effects on vibration of multilayered plates and shells. J Sound Vib 2000;225:803–29.
[34] Carrera E. A class of two dimensional theories for multilayered plates analysis. Atti. Acc. Sci. Torino 1995:49–87.
[35] Cauchy AL. Sur l'équilibre et le mouvement d'une plaque solide. Exercise Math 1828;3:381–412.
[36] Poisson SD. Mémoire sur l'équilibre et le mouvement des corps élastique. Mémoires de l'Académie des Sciences des Paris 1829;8:357–570.
[37] Kirchhoff G. Ü ber das gleichgewicht und die bewegung einer elastishen scheibe. J Reine Angew Math 1850;40:51–88.
[38] Reissner E. The effect of transverse shear deformation on the bending of elastic plates. J Appl Mech 1945;12:69–77.
[39] Mindlin RD. Influence of rotatory inertia and shear in flexural motions of isotropic elastic plates. J Appl Mech 1951;18:31–8.
[40] Carrera E, Brischetto S. Analysis of thickness locking in classical, refined and mixed multilayered plate theories. Compos Struct 2008;82:549–62.
[41] Carrera E, Brischetto S. Analysis of thickness locking in classical, refined and mixed theories for layered shells. Compos Struct 2008;85:83–90.